

Electronic Supplementary Information

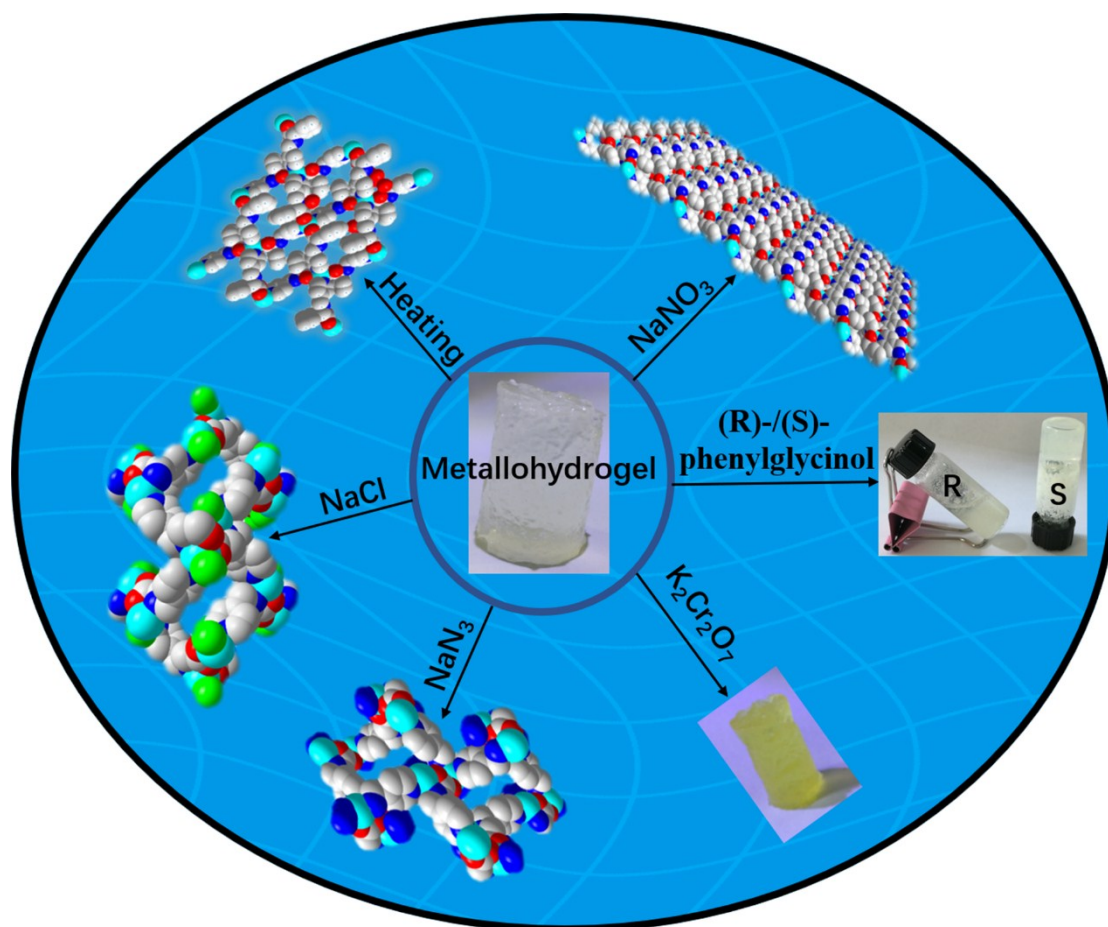
A multi-stimuli responsive metallohydrogel applied to chiral recognition, poisonous anion adsorption and construction of various chiral metal-organic frameworks

Xuebin Xu, Jiannan Xiao, Meiyang Liu and Zhiliang Liu*

Inner Mongolia Key Laboratory of Chemistry and Physics of Rare Earth Materials,
School of Chemistry and Chemical Engineering, Inner Mongolia University, Hohhot
010021, China. *Corresponding author.

Fax/ Tel: +86-471-4992261

E-mail addresses: cezlliu@imu.edu.cn (Z. L. Liu)



1. Materials and Methods

1.1 Regents: All of chemicals were purchased and used without purification. Distilled water was prepared in the laboratory and was used throughout the work.

1.2 Apparatus: Rheological measurements were performed using Physica MCR 102 (Anton Paar Instruments) equipped with a 30 mm parallel-plate geometry with a gap size of 1.0 mm. The measurement temperature was set at 25 °C. The circular dichroism spectra of the metallohydrogel was recorded on a JASCO J-810 spectropolarimeter at room temperature. Power X-ray diffraction patterns (PXRD) were obtained using crushed single crystals on an Empyrean Panalytical apparatus with Cu- K_{α} radiation ($\lambda = 1.54178\text{\AA}$). Fourier transform infrared (FT-IR) spectra were measured in the range of 4000-400 cm^{-1} using KBr pellets on PerkinElmer spectrometer. The metallohydrogel was investigated using a HITACHI S-4800 200 kV scanning electron microscope (SEM). Elemental analyses for N, C and H were obtained from a Perkin-Elmer 2400 elemental analyzer. The fluorescence excitation and emission spectra were conducted on Edinburgh Instruments FLS-920 spectrophotometer with a 450 W xenon lamp as an excitation source at room temperature. To guarantee conformity test, the slit width was kept at 3.0 nm of both excitation and the emission source. The UV-vis absorption spectra were measured using a spectrophotometer (UH-3900) in the range of 200-800 nm.

1.3 Synthesis of HL ligand

The ligand HL was prepared following reported the procedure previously reported in the literature. To an aqueous solution (20.00 mL) of (S)-Phenylglycine (15.00 mmol) and Na_2CO_3 (9.43 mmol), 4-pyridinecarboxaldehyde (15.00 mmol) was added slowly. The solution was stirred for 10 min at 80 °C. The mixture was spontaneously cooled to room temperature and then subjected to ice-bath. NaBH_4 was added slowly to the reaction mixture at 0 °C and stirred for 7h. Formic acid (98%) was then added to neutralize the excess of sodium carbonate until pH 5.0-6.0. The reaction mixture was further stirred for 1 h. The obtained white product was then filtered and dried under vacuum. Yield: 2.40 g (66.85%). The ligand has been crystallized from the aqueous

solution and utilized for its characterization. Elemental analysis (%) calcd for $C_{14}H_{14}N_2O_2$: C, 69.42, H, 5.79, N, 11.57; found C, 69.27, H, 5.69, N, 11.49. IR (KBr, cm^{-1}): 3436 (vs), 3024 (m), 2829 (m), 2389 (w), 1614 (s), 1565 (s), 1472 (m), 1435 (m), 1414 (m), 1381 (s), 1261 (w), 1180 (w), 1077 (w), 1028 (m), 1066 (w), 984 (w), 848 (m), 789 (m), 745 (m), 691 (s), 615 (s), 593 (m), 507 (m).

1.4 Synthesis of the metallohydrogel

0.5 mL of aqueous solution of zinc acetate (0.20 mmol) was mixed with 0.7 mL aqueous solution of ligand (0.35 mmol) in a tightly capped 5 mL vial followed by sonication affording the immediate formation of metallohydrogel.

1.5 The transformation of metallohydrogel to Zn-MOFs-1

The metallohydrogel was kept for at 90 °C for 30 h, and then cooled down to room temperature at a rate of 5 °C /h. Colorless rod crystals which were insoluble in water were collected by filtration, washing with water and finally dried at ambient temperature. Zn-MOFs-1, Yield: 49%, based on metal salt. Elemental analysis (%) calcd for $C_{28}H_{26}ZnN_4O_4$: C, 61.43, H, 4.75, N, 10.24; found C, 61.28, H, 4.68, N, 10.15. IR (KBr, cm^{-1}): 3371 (vs), 3079 (w), 3046 (w), 2926 (w), 2796 (m), 1961 (w), 1614 (s), 1456 (m), 1429 (s), 1386 (s), 1348 (m), 1310 (w), 1256 (w), 1229 (m), 1180 (w), 1142 (m), 1060 (m), 1028 (m), 936 (m), 876 (s), 811 (s), 762 (m), 724 (s), 691 (m), 621 (w), 599 (w).

1.6 Anion induced metallohydrogel-crystal conversion

NaX salt ($X = Cl^-$, N_3^- and NO_3^-) was sprinkled over the top of metallohydrogels with 1:1 stoichiometric ratio and completely converts into MOFs crystals for 7 days. Heating can accelerate the conversion of the metallohydrogel to crystals, under high-temperature conditions (90 °C), the conversion was successful in 48 hours.

Zn-MOFs-2, Yield: 40%, based on HL. Elemental analysis (%) calcd for $C_{14}H_{13}ZnClN_2O_2$: C, 49.11, H, 3.80, N, 8.19; found C, 48.95, H, 3.80, N, 8.15. IR (KBr, cm^{-1}): 3436 (vs), 3187 (m), 3046 (w), 2916 (w), 1624 (s), 1592 (m), 1548 (m), 1484 (w), 1457 (m), 1418 (s), 1348 (m), 1278 (w), 1212 (m), 1120 (m), 1071 (m), 1022 (m), 1006 (m), 968 (w), 925 (m), 860 (w), 811 (s), 751 (m), 708 (m), 637 (m), 539 (m).

Zn-MOFs-3, Yield: 42%, based on HL. Elemental analysis (%) calcd for $C_{14}H_{13}ZnN_5O_2$: C, 48.18, H, 3.73, N, 20.08; found C, 48.08, H, 3.73, N, 19.93. IR (KBr, cm^{-1}): 3409 (vs), 3182 (s), 3035 (w), 2943 (w), 2861 (m), 2069 (s), 1630 (s), 1586 (m), 1484 (m), 1451 (s), 1418 (m), 1348 (m), 1288 (m), 1217 (m), 1185 (w), 1136 (m), 1071 (m), 1006 (m), 963 (m), 919 (m), 854 (w), 816 (s), 789 (m), 740 (m), 702 (m), 637 (s), 551 (m).

Zn-MOFs-4, Yield: 46%, based on HL. Elemental analysis (%) calcd for $C_{28}H_{32}ZnN_6O_{12}$: C, 47.32, H, 4.51, N, 11.83; found C, 47.31, H, 4.49, N, 11.76. IR (KBr, cm^{-1}): 3480 (vs), 3361 (s), 3057 (w), 2937 (w), 2845 (w), 2780 (m), 1966 (w), 1619 (s), 1435 (m), 1381 (s), 1310 (m), 1223 (w), 1180 (w), 1136 (m), 1055 (m), 1028 (m), 941 (m), 805 (s), 762 (m), 718 (s), 696 (m), 621 (w), 593 (w).

1.7 Fabrication of metallohydrogel films

The preparation process comprises the following steps: (1) casting the metallohydrogel films with thickness of 1.0 mm on a glass plate using a casting knife; (2) Immediately immersing the cast films in carbon tetrachloride and being dried at room temperature.

1.8 The interaction of the metallohydrogel with chiral phenylglycinol

(1) 0.5 mL of aqueous solution of zinc acetate (0.022 g) was mixed with 0.5 mL of aqueous of solution of ligand (0.0275 g) in a tightly capped 5.0 ml vial followed by sonication affording the immediate formation of metallohydrogel (27.5 g/L); (2) A solution of (R)-phenylglycinol (0.0623 g), a solution of (S)-phenylglycinol (0.0623 g), or a solution of the mixture (0.0623 g) with different molar ratios at 1:1, 2:1, 3:1 and 4:1 of (R)-phenylglycinol and (S)-phenylglycinol in the distilled water (0.5 mL) was added to the surface of metallohydrogel; (3) Ultrasonic agitation for 2 min. The experiment results show as follows: (1) When (S)-phenylglycinol was added to the surface of metallohydrogel, it remained stable, whereas gel collapsing and precipitation was observed for (R)-phenylglycinol under identical conditions; (2) When the mixture solution of (R)-phenylglycinol and (S)-phenylglycinol was added, the metallohydrogel collapsing and precipitation can be observed only at (R)-phenylglycinol/(S)-phenylglycinol molar ratio of 4:1.

1.9 Anions interference experiments

(1) 0.5 mL of different concentrations (0.5, 1.0 and 1.5 M) of NaCl, NaN₃ and NaNO₃ were added to metallohydrogel with the concentration of 55.0 g/L in a tightly capped 5.0 ml vial followed by sonication. when 0.5M and 1.0 M of NaCl, NaN₃, and NaNO₃ were added, the metallohydrogel remained stable. The metallohydrogel collapsing and precipitation was observed until the anion concentration up to 1.5 M; (2) A solution of (R)-/(S)-phenylglycinol (0.36 mmol) in the distilled water (0.5 mL) was added to the surface of metallohydrogel containing 0.5 M of anions; (3) Ultrasonic agitation for 2 min.

2. Characterization of the metallohydrogel

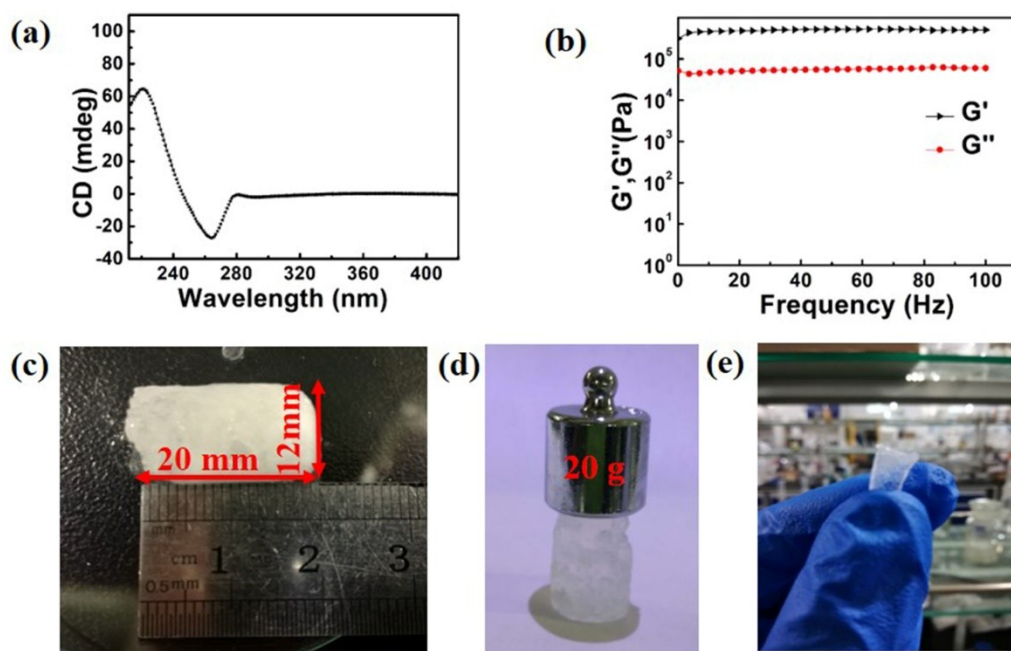


Fig. S1 The metallohydrogel of physical properties: (a) CD spectra for the metallohydrogel at RT (b) dynamic frequency sweep test at strain = 0.1% (c) the length and diameter of the metallohydrogel (d) bearing a load of 20 g chromed steel weight (e) film of the metallohydrogel.

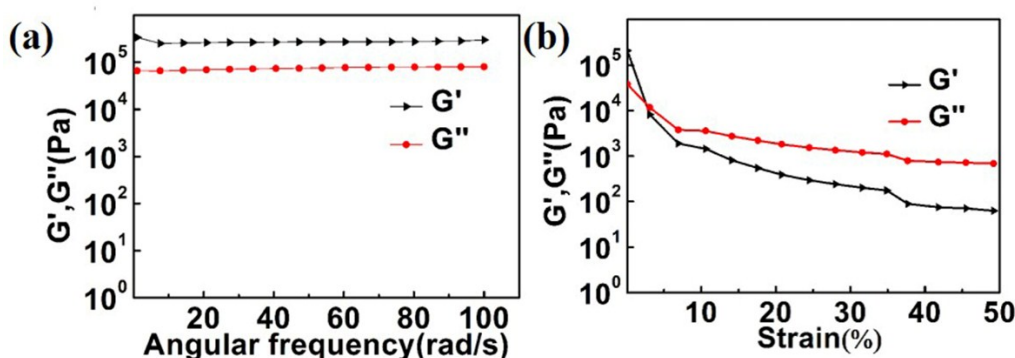


Fig. S2 (a) Angular frequency sweep test at strain = 0.1% (b) Dynamic strain sweep test at a constant

frequency of 1 Hz.

3. X-ray-Crystallography (Single-crystal diffraction) and Characterization of MOFs

3.1 Crystal Data Collection and Refinement

Crystallographic data were collected at a temperature of 293(2) K on a Bruker Apex II CCD diffractometer with graphite mono chromated Mo- K_{α} radiation ($\lambda = 0.71073 \text{ \AA}$). The structures were solved by direct methods and refined using SHELXTL suite of programs. All non-hydrogen atoms were refinement anisotropically. The H atoms were introduced in calculated positions and refined with fixed geometry with respect to their carrier atoms. CCDC 1936598, 1936603, 1936604 and 1936605 contained the supplementary crystallographic data for this paper.

3.2 Crystallographic structural parameters of MOFs

Table S1. Crystallographic structural parameters of MOFs

MOFs	Zn-MOFs-1	Zn-MOFs-2	Zn-MOFs-3	Zn-MOFs-4
CCDC	1936598	1936604	1936603	1936605
Empirical formula	C ₂₈ H ₂₆ ZnN ₄ O ₄	C ₁₄ H ₁₃ ZnClN ₂ O ₂	C ₁₄ H ₁₃ ZnN ₅ O ₂	C ₂₈ H ₃₂ ZnN ₆ O ₁₂
Formula weight	547.90	342.08	348.66	709.96
Temperature	293(2) K	293(2) K	293(2) K	293(2) K
Wavelength	0.71073 Å	0.71073 Å	0.71073 Å	0.71073 Å
Crystal system	Orthorhombic	Orthorhombic	Orthorhombic	Orthorhombic
space group	<i>P</i> 2 ₁ 2 ₁ 2	<i>P</i> 2 ₁ 2 ₁ 2 ₁	<i>P</i> 2 ₁ 2 ₁ 2 ₁	<i>P</i> 2 ₁ 2 ₁ 2 ₁
<i>a</i>	13.8396(14) Å	7.5321(12) Å	7.860(3) Å	12.246(3) Å
<i>b</i>	15.5527(16) Å	12.861(2) Å	13.271(5) Å	14.757(3) Å
<i>c</i>	5.7751(6) Å	14.071(2) Å	13.788(5) Å	17.563(3) Å
Volume	1243.1(2) Å ³	1363.1(4) Å ³	1438.3(10) Å ³	3174.0(11) Å ³
<i>Z</i>	2	4	4	4
Calculated density	1.464 Mg/m ³	1.667 Mg/m ³	1.610 Mg/m ³	1.486 Mg/m ³
Absorption coefficient	1.031 mm ⁻¹	1.999 mm ⁻¹	1.722 mm ⁻¹	0.846 mm ⁻¹
<i>F</i> (000)	568.0	696.0	712.0	1472.0
Theta range for data collection	1.970 - 25.018°	3.134 - 28.411 °	2.130 - 24.999 °	1.802 - 25.018 °
Reflections collected	13193	18599	14824	17932
Independent reflections	9583	3422	2545	5593
Completeness to theta= 25.00°	[<i>R</i> (int)=0.0302]	[<i>R</i> (int)=0.0378]	[<i>R</i> (int)=0.0718]	[<i>R</i> (int)=0.0725]
Refinement method	Full-matrix least-squares on <i>F</i> ²	Full-matrix least-squares on <i>F</i> ²	Full-matrix least-squares on <i>F</i> ²	Full-matrix least-squares on <i>F</i> ²
Data/restraints/parameters	2186 / 0 / 169	3422 / 0 / 182	2545 / 0 / 200	5593 / 6 / 435
Goodness-of-fit on <i>F</i> ²	1.208	1.039	1.076	1.027
Flack parameter	0.03(2)	0.031(16)	0.02(3)	0.02(3)
Final <i>R</i> indices [<i>I</i> >2σ(<i>I</i>)]	<i>R</i> ₁ = 0.0276, <i>wR</i> ₂ = 0.0826	<i>R</i> ₁ = 0.026, <i>wR</i> ₂ = 0.0569	<i>R</i> ₁ = 0.0363, <i>wR</i> ₂ = 0.0761	<i>R</i> ₁ = 0.0567, <i>wR</i> ₂ = 0.1332
<i>R</i> indices (all data)	<i>R</i> ₁ = 0.0281, <i>wR</i> ₂ = 0.0828	<i>R</i> ₁ = 0.035, <i>wR</i> ₂ = 0.0592	<i>R</i> ₁ = 0.0492, <i>wR</i> ₂ = 0.0822	<i>R</i> ₁ = 0.0900, <i>wR</i> ₂ = 0.1513
Largest diff. peak and hole	0.493 and -0.324 e. Å ⁻³	0.272 and -0.309 e. Å ⁻³	0.462 and -0.313 e. Å ⁻³	0.538 and -0.587 e. Å ⁻³

3.3 Crystallographic details of the as-synthesized MOFs

Zn-MOFs-1 was directly synthesized by the metallohydrogel, and Zn-MOFs-2, Zn-MOFs-3 and Zn-MOFs-4 were synthesized by layering the metallohydrogel with solid salt. Interestingly, Zn-MOFs-2, Zn-MOFs-3 and Zn-MOFs-4 crystallize in the $P2_12_12_1$ space group where Zn-MOFs-1 in a $P2_12_12$ space group, respectively.

3.3.1 Molecular structure of Zn-MOFs-1

In Zn-MOFs-1, the Zn(II) center is four-coordinated by two pyridine N atoms from two HL ligands, two oxygen atoms deriving from two different carboxylate oxygen atoms of HL ligands. The Zn(II) center exhibits a distorted tetrahedral coordination geometry, chelated by $O_{\text{carboxylate}}$ and pyridyl group. The average bond distance of Zn–N is 2.027 Å, and the average bond distance of Zn–O is 1.989 Å; the O–Zn–O and O–Zn–N angles are 100.944° and 122.514°, respectively. The adjacent Zn(II) ions are bridged by carboxylate groups and one pyridyl group of the bridging ligand HL, extending the structure into a 2D framework.

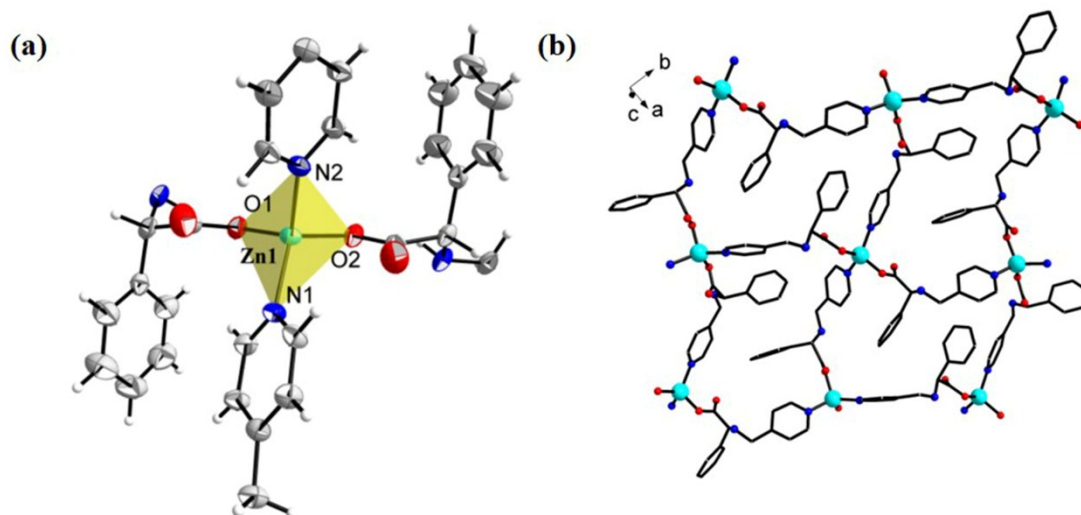


Fig. S3 Molecular structure of the as-synthesized Zn-MOFs-1 (parts of H atoms were omitted for clarity).

3.3.2 Molecular structure of Zn-MOFs-2 and Zn-MOFs-3

Zn-MOFs-2 and Zn-MOFs-3 are two isostructural three dimensional MOFs. The Zn(II) center adopts a distorted square-pyramidal geometry ($\tau = 0.467$ and 0.457). The Zn(II) center is five-coordinated by carboxylate oxygen atom (O1), pyridyl group, protonated N_{amine} and introduced chloride anion or azide anion, thus forms an NO_2X ($\text{X} = \text{Cl}$ or

N_{azide} plane. The axial coordination is served by carboxylate oxygen atom (O2). Two adjacent crystallographically equivalent Zn(II) atoms are connected by the bidentate chelating carboxylate groups from the HL ligands, extending the structure into 3D framework. The distance between the two equivalent Zn(II) centers is 5.4410(16) Å.

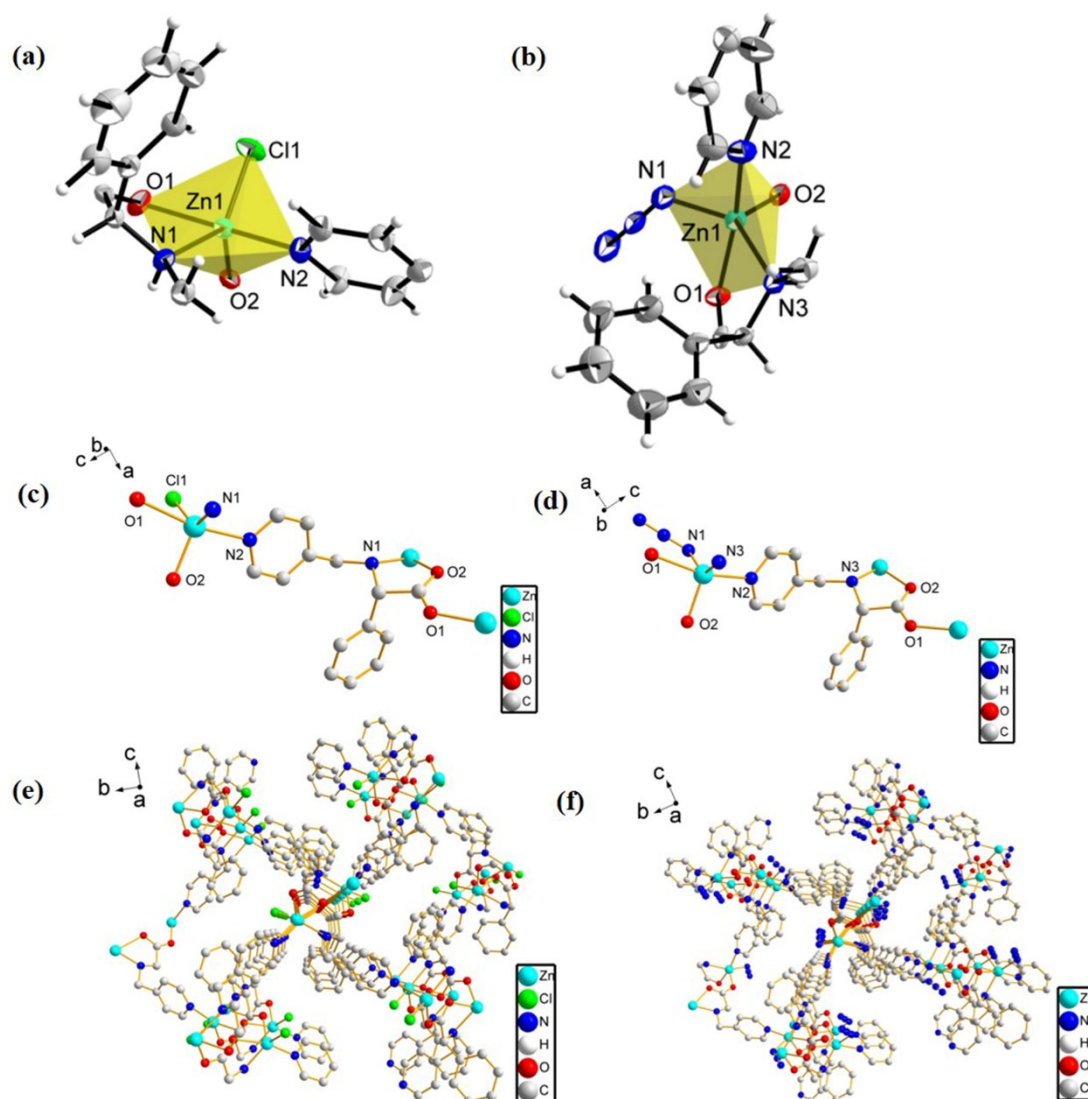


Fig. S4 Molecular structures of the as-synthesized Zn-MOFs-2 and Zn-MOFs-3 (parts of H atoms were omitted for clarity).

3.3.3 Molecular structure of Zn-MOFs-4

In Zn-MOFs-4, the Zn(II) center exhibits a distorted tetrahedral coordination geometry. The Zn(II) center is four-coordinated by two pyridine N atoms from two different HL ligands, two oxygen atoms deriving from carboxyl oxygen atoms, extending the structure into a 2D framework. Zn-MOFs-4 shows different binding modes, where

uncoordinated NO_3^- lies within the pore cavity. From elemental analysis, we assign the remaining positive charge to be a hydronium ion, H_3O^+ .

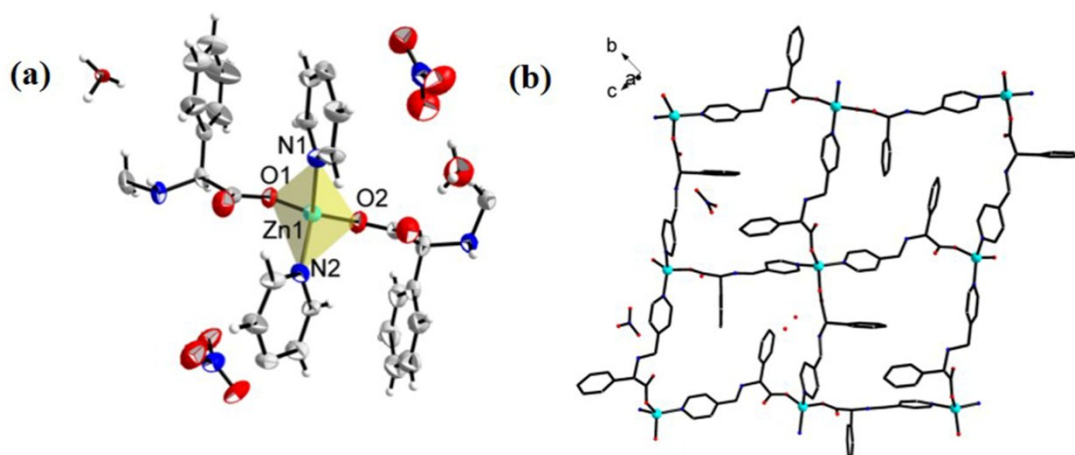


Fig. S5 Molecular structure of the as-synthesized Zn-MOFs-4 (parts of H atoms were omitted for clarity).

3.4 Selected bond lengths (Å) and geometry index values

Table S2. Selected bond lengths (Å) and geometry index values

Zn-MOFs	Zn-NH _{amine}	Zn-N _{pyridine}	Zn-Cl/N ₃	Zn-O ₁ _{carboxylate}	Zn-O ₂ _{carboxylate}	geometry index (τ)
1	-	2.0268(32)	-	1.9893(28)	-	-
2	2.1378(26)	2.1373(27)	2.2717(11)	1.9832(23)	2.3038(24)	0.467
3	2.0803(41)	2.1326(55)	1.9760(55)	1.9744(39)	2.3066(41)	0.457
4	-	2.0102(62)	-	1.9721(60)	1.9585(60)	-
		2.0088(66)				

3.5 Characterization of MOFs

The phase purity of the crystals of MOFs was confirmed by the high similarity between the experimental and simulated PXRD patterns.

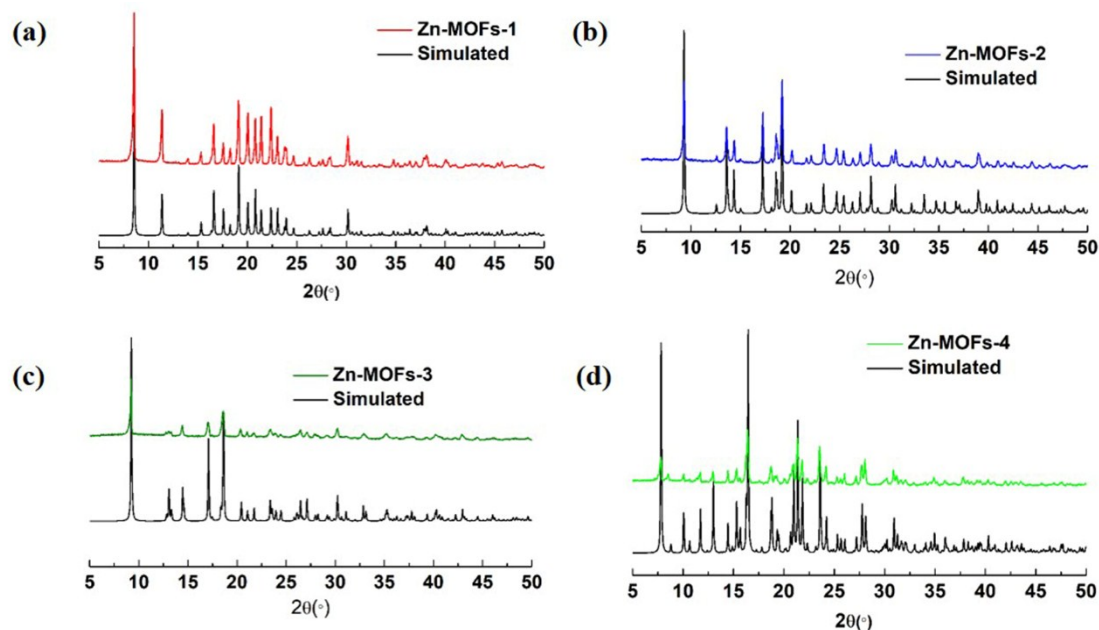


Fig. S6 PXRD patterns of as-synthesis sample and the simulated spectra from single-crystal data.

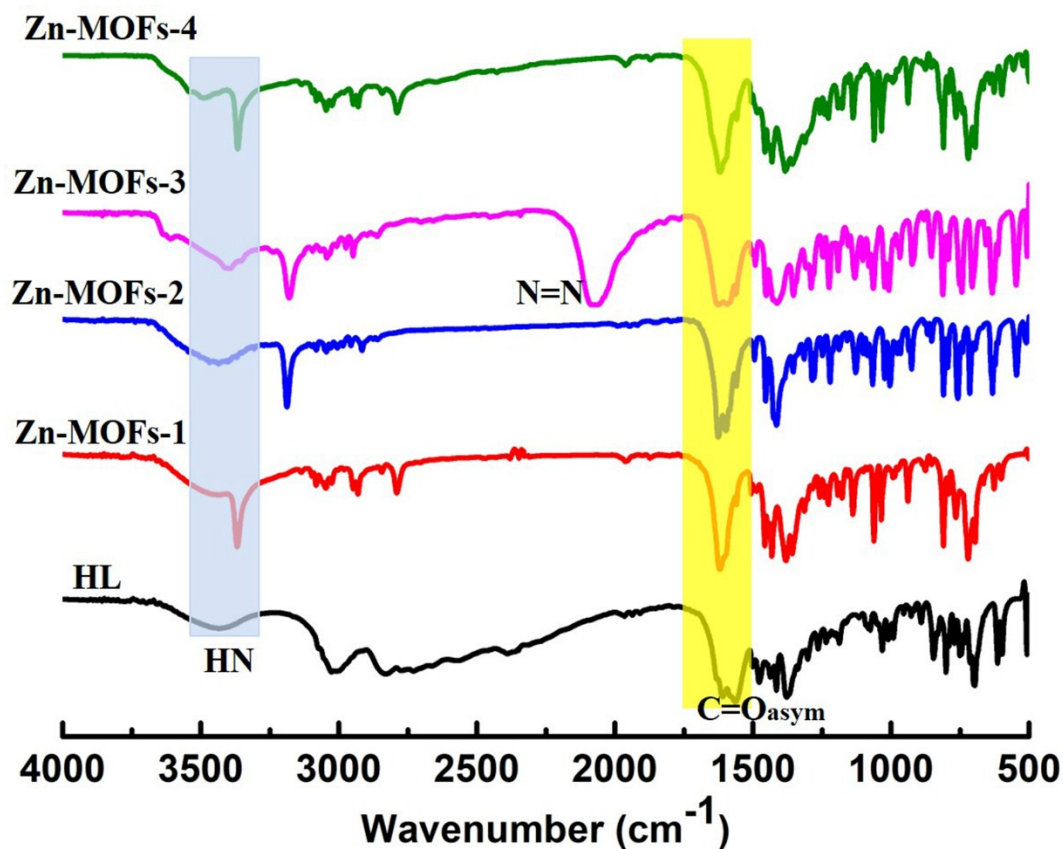


Fig. S7 FTIR spectra of HL, Zn-MOFs-1, Zn-MOFs-2, Zn-MOFs-3 and Zn-MOFs-4.

4. Studies on the sensing mechanisms

4.1 The interaction of the metallohydrogel with (R)/(S)-phenylglycinol

Experimental procedures for the fluorescence study of metallohydrogel in the presence

of chiral amino alcohols: to a solution of Zn-MOFs-1 (6.0×10^{-4} M, 3 mL) was sequentially added 10, 20, 30 and 40 equivalents of an amino alcohol. Each sample was sonicated for 1min before the fluorescence measurement.

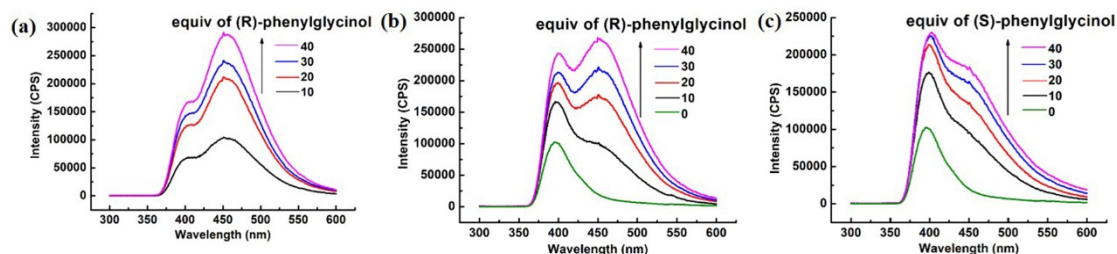


Fig. S8 The excitation and emission spectra of (a) Fluorescence spectra of $\text{Zn}(\text{OAc})_2 \cdot 2\text{H}_2\text{O}$ (6.0×10^{-4} M) toward (R)-phenylglycinol at 10, 20, 30 and 40 equiv (b) Fluorescence spectra of Zn-MOFs-1 (6.0×10^{-4} M) toward (R)-phenylglycinol at 0, 10, 20, 30 and 40 equiv (c) Fluorescence spectra of Zn-MOFs-1 (6.0×10^{-4} M) toward (S)-phenylglycinol at 0, 10, 20, 30 and 40 equiv.

4.2 The interaction of the metalhydrogel with the mixture of (R)-phenylglycinol and (S)-phenylglycinol

The fluorescence sensing experiments of Zn-MOFs-1 to the mixture of (R)- and (S)-phenylglycinol were performed.

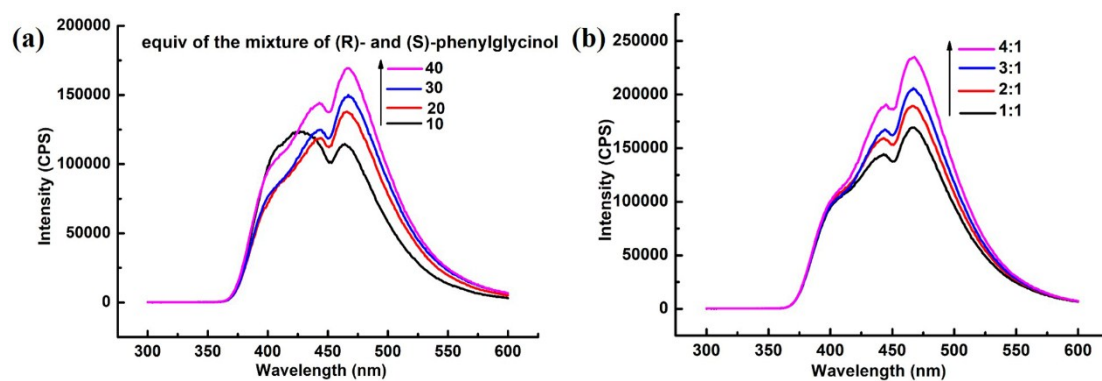


Fig. S9 (a) Fluorescence spectra of Zn-MOFs-1 (6.0×10^{-4} M) toward the mixture of (R)- and (S)-phenylglycinol (with a ratio at 1:1) at 10, 20, 30 and 40 equiv (b) Fluorescence spectra of Zn-MOFs-1 (6.0×10^{-4} M) toward the mixture of (R)- and (S)-phenylglycinol (with a ratio at 1:1, 2:1, 3:1 and 4:1) at 40 equiv.

4.3 Results of anions interference experiments

The stability of metalhydrogel was assessed in the presence of both anions (0.5 M) and (R)-/(S)-phenylglycinol (0.36 mmol). The metalhydrogel occurred collapsing and

precipitation in the presence of (R)-phenylglycinol, while the metallohydrogel still remained stable in the presence of (S)-phenylglycinol. This result shows that the metallohydrogel also can recognize (R)-phenylglycinol under the interference of a certain concentration of anions.

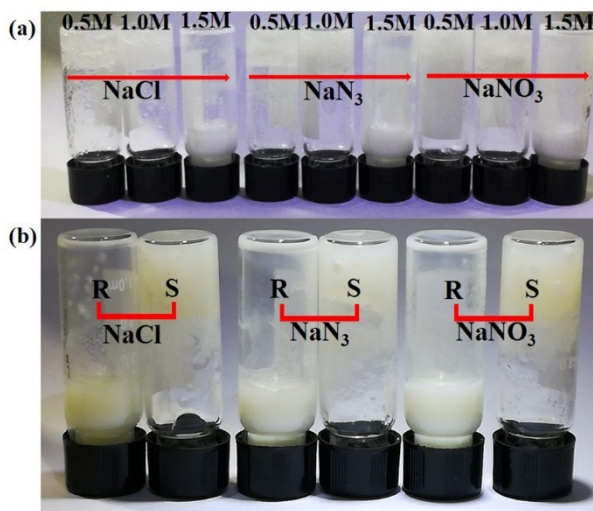


Fig. S10 (a) the morphology of metallohydrogel after adding different concentrations of anions; (b) the morphology of metallohydrogel after adding (R)-phenylglycinol (0.36 mmol) or (S)-phenylglycinol (0.36 mmol) in presence of anions (0.5 M).

5. The gelation mechanism

It can be obviously observed that the morphologies of the metallohydrogel and the Cr(VI)-adsorbed metallohydrogel are different. The phenomenon should be caused by the hexavalent Cr(VI) species, which are taken up into the metallohydrogel, and the abundant porous structures are formed. Conversely, the morphologies of fibers and Zn-MOFs-1 have no obvious change after adsorbing and enriching hexavalent Cr(VI) species. This phenomenon indicates that Cr(VI) species can adjust the morphologies of metallohydrogel in the early stage of metallohydrogel, but can not affect the growing of metallohydrogel in the late stage.

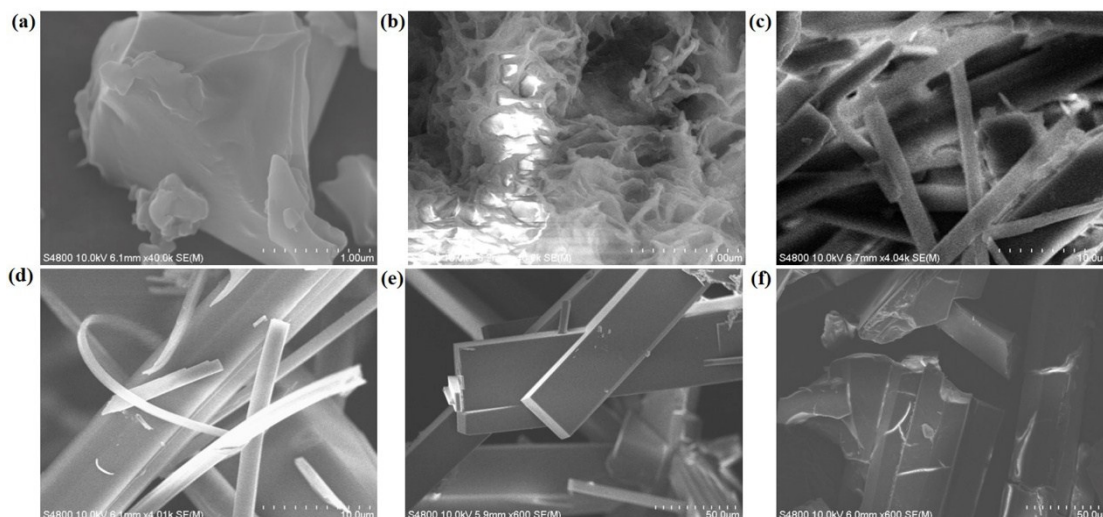


Fig. S11 The SEM images of (a) the metalhydrogel (b) the Cr(VI)-adsorbed metalhydrogel (c) the fibers of the metalhydrogel after aging for 1h at 60°C (d) the fibers of the Cr(VI)-adsorbed metalhydrogel after aging for 1h at 60°C (e) Zn-MOFs-1 (f) Zn-MOFs-1 synthesized by Cr(VI)-adsorbed metalhydrogel.

6. Adsorption of hexavalent Cr(VI)

The concentration of Cr(VI) was measured by the diphenyl-carbazide colorimetric method at 540 nm using UV-vis spectroscopy.^[1,2]

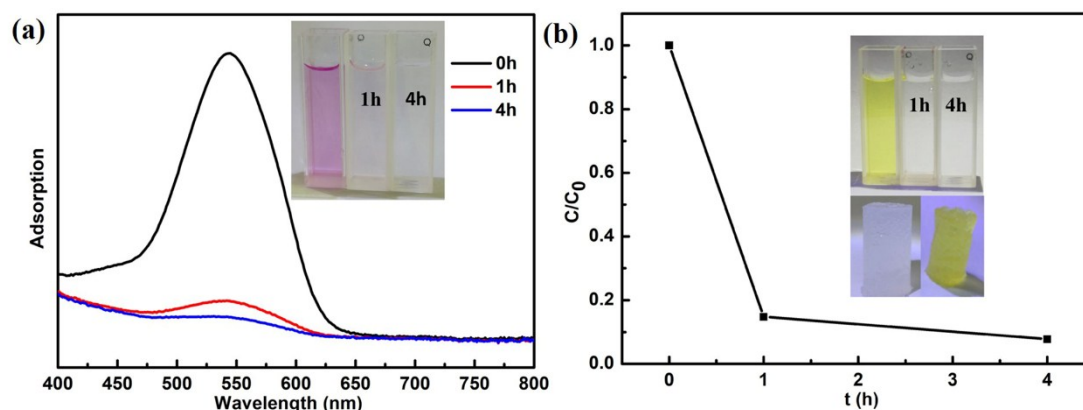


Fig. S12 (a) The UV spectra of $K_2Cr_2O_7$ solution before and after adsorption (b) The adsorption activity toward hexavalent Cr(VI).

References

- 1 R. Zhao, X. Zhang, Y. Su, Z. L. Liu and C. Du, *Chem. Eng. J.*, 2020, 380, 122432.
- 2 L. Yang, X. Zheng, M. Liu, S. Luo, Y. Luo and G. Li, *J. Hazard. Mater.*, 2017, 329, 230.